

Supplemental information

**BAFFR activates PI3K/AKT signaling in human naive
but not in switched memory B cells through direct
interactions with B cell antigen receptors**

Eirini Sevdali, Violeta Block, Marie Lataretu, Huiying Li, Cristian R. Smulski, Jana-Susann Briem, Yannic Heitz, Beate Fischer, Neftali-Jose Ramirez, Bodo Grimbacher, Hans-Martin Jäck, Reinhard E. Voll, Martin Hölzer, Pascal Schneider, and Hermann Eibel

Supplemental Figures

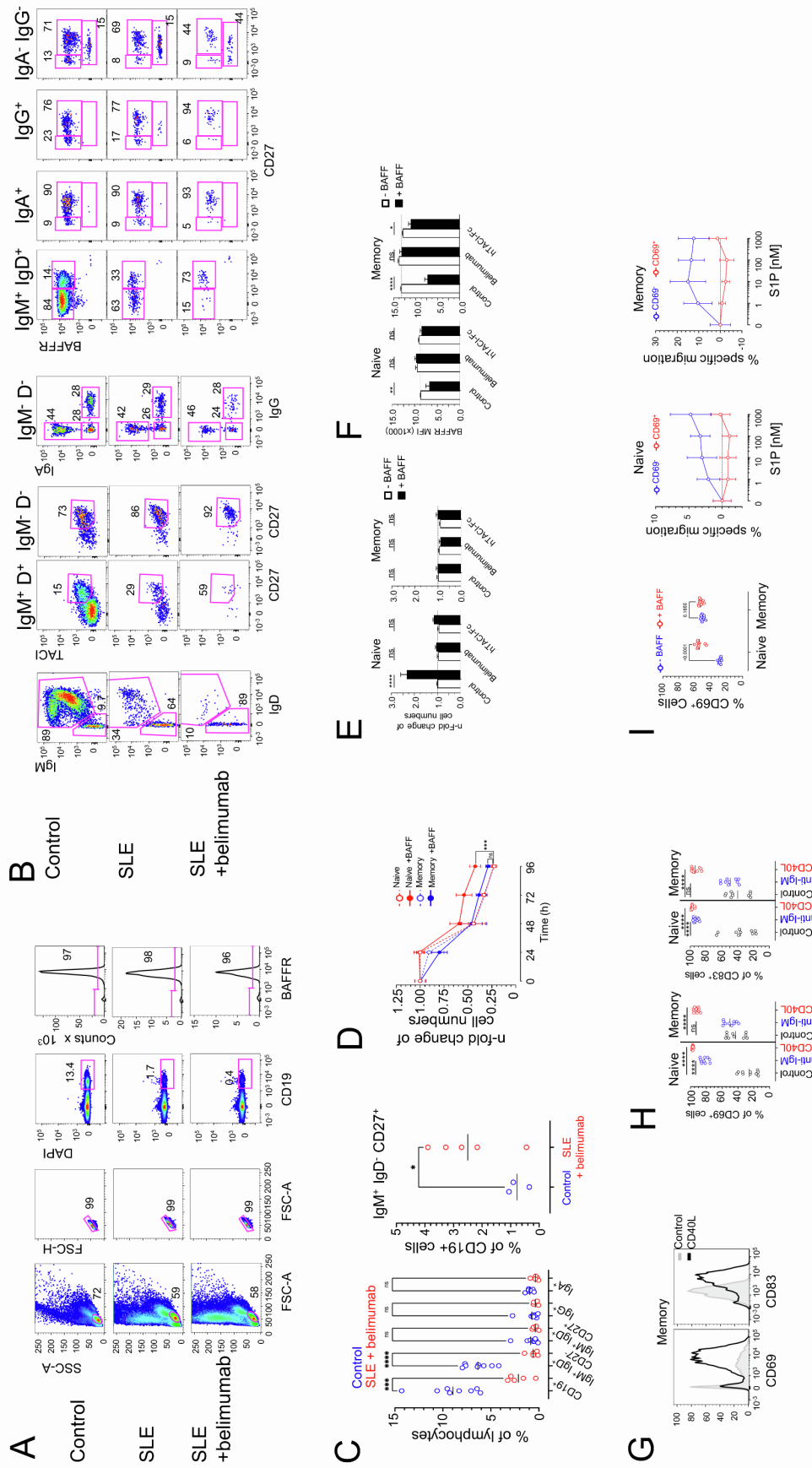


Figure S1 (related to Figure 1). Phenotype, BAFF-dependent survival and activation of B cell subsets.

A. Gating strategy applied in flow cytometric analyses. The representative example shows lymphocyte populations of peripheral blood mononuclear cells (PBMCs) from a healthy donor (control), a SLE patient (SLE) and a SLE patient treated for > 1 year with belimumab as identified by the forward (FSC-A) and the side scatter (SSC-A) reflecting the small size and low granularity of these cells. Within the lymphocyte population, single cells were gated by the FSC-A (area) and FSC-H (height). Living B cells were defined as CD19⁺ DAPI⁻ cells, of which > 96% expressed BAFFR.

B. B cell subsets. The CD19⁺ cells of the control, SLE and SLE + belimumab samples were analyzed for the expression of IgM, IgD, CD27, BAFFR, TACI, IgA and IgG. The IgM⁺ IgD⁺ subset included naive (IgD⁺ CD27⁻) and marginal zone B cells (IgD⁺ CD27⁺). The latter expressed TACI on their cell surface. Most of the IgM⁻ IgD⁻ cells were switched memory B cells (MBCs) expressing IgA (IgA⁺, 42 - 46%) or IgG (IgG⁺, 28 - 29%), CD27 and TACI (73 - 92%). CD19⁺ IgM⁻ IgD⁻ IgG⁻ IgA⁻ cells (24 - 28%) were BAFFR⁺ (53 - 84%) or BAFFR^{low/+} CD27^{low/+} (15 - 44%).

C. Memory B cells persist in belimumab-treated SLE patients. Lymphocytes of controls and SLE patients who were treated with belimumab for > 6 months were gated as shown in panels A and B and analyzed by flow cytometry for the expression of CD19, CD27, IgM, IgD, IgG, and IgA. The plot on the left compares the percentages of B cells and B cell subsets in lymphocytes of controls (n=8) and belimumab-treated SLE patients (n=5). Controls have significantly more CD19⁺ B cells and CD19⁺ IgD⁺ CD27⁻ naive B cells than SLE patients treated for > 6 months with the BAFF-neutralizing mAb belimumab. The plot on the right side

shows the percentages of IgM⁺ IgD⁻ CD27⁺ memory B cells in controls (n=3) and in the SLE patients (n=5). Statistically significant differences between controls and patients were calculated applying Brown-Forsythe and Welch's ANOVA assuming unequal SD with Dunnett T3 correction for multiple comparisons with n<50. (*p≤0.0332; **p≤0.0021; ***p≤0.0002; **** p<0.0001; ns, not significant).

D. BAFF-induced survival in naive and memory B cells. B cells were stimulated with BAFF (20 ng/ml) for 4 sequential days and analyzed by flow cytometry and timed acquisition. N-fold changes of cell numbers were calculated as [cell number at each day ±BAFF /cell number –BAFF at day 0]. Plots show the mean and SD of 2 independent experiments (3 replicates/experiment) with two healthy donors (HD); ***p<0.001; ns, not significant (Kruskal-Wallis with Dunn's multiple comparisons test).

E. B cells do not produce endogenous BAFF. BAFF (20 ng/mL) was mixed with belimumab (1 µg/mL), hTACI-Fc (100 ng/mL) or medium (control) and incubated at room temperature for 1 day. B cells were then incubated with BAFF ±belimumab or ±TACI-Fc for 3 days or without the ligand, and cell numbers were analyzed by flow cytometry and timed acquisition. N-fold changes in cell numbers were calculated as [cell number ± BAFF ± inhibitor]/[cell number without BAFF without inhibitor]. The plots show the mean ±SEM of n-fold change of cell counts of each B cell subset from two independent experiments with samples from two different HD. ****p<0.0001; ns, not significant (2-way Anova with Tukey multiple comparisons test).

F. Belimumab and hTACI-Fc block BAFF binding to BAFFR. Median fluorescence intensity (MFI) of BAFFR surface expression of naive and memory B cell subsets shown in (E) at day 3 using the anti-BAFFR monoclonal antibody

11C1. The antibody binds to BAFFR only when BAFFR is not occupied by BAFF. The plot shows the mean \pm SEM of BAFFR MFI from two independent experiments with two different HD; **** $p < 0.0001$; ** $p < 0.01$; * $p < 0.05$; ns, not significant (2-way Anova with Tukey multiple comparisons test).

G. CD40L induces CD69 and CD83 expression in memory B cells. Histogram overlays show changes in CD69 and CD83 expression by MBCs activated with CD40L overnight. The histogram plots are representative of 6 independent experiments with B cells from different healthy donors.

H. Anti-IgM and CD40L differentially activate CD69 and CD83 expression in naive and memory B cells. CD40L induces CD69 and CD83 expression on the surface of naive and of MBCs, while anti-IgM activates only naive B cells. B cells were incubated overnight with anti-IgM (2 μ g/mL) or CD40L or left untreated and analyzed by flow cytometry. Plot shows the mean of pooled data from 6 independent experiments with B cells from different HD. **** $p < 0.0001$; ns, not significant (2-way Anova with Tukey multiple comparisons test).

I. BAFF-induced CD69 inhibits S1P-dependent B cell migration. B cells were cultivated overnight with BAFF or left untreated. The migration against S1P was then analyzed in transwell assays with different concentrations of S1P in the lower well. Cells in upper and lower wells were analyzed by flow cytometry for the expression of IgD, CD27 and CD69. The fraction of sessile or migrating cells was determined by timed acquisition. The percentage of migrating cells was calculated as $[\text{number of cells isolated from the lower well}] / [\text{number of cells retrieved from the upper well}] \times 100$. The transwell migration assay was performed with two biological and two technical replicates. Plots show mean values \pm SD. Statistical significances in CD69 expression between naive and

memory B cells were calculated by 2-way ANOVA with Tukey multiple comparisons test.

Figure S2 (related to Figure 2). Gene expression patterns.

A. Normalized counts of transcripts in naive and memory B cells. The box plots show transcripts of genes expressed typically by naive and MBCs, or by plasma cells. IGHM and IgHD are expressed by naive and MZ B cells, the H-chain genes of the switched isotypes (IGHG1 – IGHG4, IGHA1, IHGA2) by memory B cells, BAFFR is expressed by all B cells, CD23 preferentially by naive B cells, CD27, TACI and Fas by memory B cells, BCMA and PRDM1 are expressed by plasma cells. The box plots represent normalized gene expression values showing the spread as boxes, the mean as lines (numerical values) and the individual values as dots.

B. Scatter plot of RNA-seq expression analysis. The scatter plot shows log₂ fold-changes in response to BAFF of differentially expressed genes present in both comparisons (naive B cells +BAFF vs naive B cells –BAFF vs memory B cells –BAFF vs naive B cells –BAFF). Significant differentially expressed genes adjusted to p-values <0.1 in both comparisons are colored in red. Green and blue show transcripts that are expressed with significant differences in only one comparison, memory B cells –BAFF vs naive B cells –BAFF, and naive B cells +BAFF vs naive B cells –BAFF, respectively.

C. Volcano plots of the RNA-seq expression analysis. Volcano plot representation of genes significantly regulated by BAFF in naive (left) and in memory B cells (right); log-fold-change threshold = 0.9, adjusted p-value = 0.1.

D. Functional (indirect) and direct interactions of genes upregulated by BAFF in naive B cells. The networks showing interactions between genes induced or repressed were generated with STRING, a database of known and

predicted protein-protein interactions (<https://www.string-db.org>). The parameters were set for full networks based on evidence (textmining, experiments, databases, co-expression) applying a high confidence score of 0.70. Clusters were calculated by K-means clustering to a specific number of 5.

E. Functional (indirect) and direct interactions of genes downregulated by BAFF in naive B cells. The networks were identified by STRING as described in panel D.

F. BAFF-induced change in the expression of chemokines and interleukins. Purified B cells were incubated for 2 days with BAFF (20 ng/mL) or left untreated and analyzed for the expression of CCL3, CCL4, IL-1 β , IL-6 and IL-10 by intracellular flow cytometry.

G. BAFF induces IL-21R expression on naive B cells and stimulates proliferation in the presence of IL-21. B cells were labelled with cell-trace violet (CTV) and stimulated with BAFF, CD40L or left untreated for 4 days. The plot shows the MFI of IL21R surface expression in naive and MBCs from 2 independent experiments (left). The percentage of dividing cells was calculated by the dilution of CTV by B cells treated for 2 days with BAFF or CD40LG followed by the addition of IL-21 for 2 days. The histogram inserts show the dilution of the CTV label after 4 days of cultivation. Black histogram = control, red = BAFF + IL-21, blue = CD40L + IL-21.

Figure S3 (related to Figure 3). BAFFR signaling in naive and switched memory B cells.

A. Inhibition of NIK blocks BAFF-induced NF- κ B2 processing in primary B cells.

B cells were incubated with increasing concentrations of the cell-permeable NIK inhibitor SMI1 for 1 h before adding BAFF (20 ng/mL). After overnight incubation, whole extracts were analyzed by immunoblotting for the NIK-dependent processing of NF- κ B2 p100 precursor into p52. The percentage of NF- κ B2 processing (% p100 processing) was calculated after densitometric analysis of the western blot images as $[100 \times (\text{p52 signal})/(\text{p52}+\text{p100 signal})][+\text{BAFF}] - 100 \times (\text{p52 signal})/(\text{p52}+\text{p100 signal})[\text{w/o BAFF}]$.

B. BAFF-induced S6 phosphorylation differs between naive and memory B cells.

Peripheral blood mononuclear cells (PBMCs) were treated with increasing concentrations of BAFF for 1 h and the phosphorylation of S6 (S240/244) was assessed by intracellular flow cytometry. The diagram displays mean percentage \pm SEM of pS6⁺ cells within the naive and memory B cell subsets of two healthy donors.

C. Comparison of S6 phosphorylation induced by BAFF, anti-IgM or CD40L.

PBMCs were treated with BAFF, F(ab')₂ anti-IgM (2 μ g/mL) or CD40L for 1 h and analyzed for the phosphorylation of S6 (S240/244) as described in (B). The plot shows the mean of pS6⁺ cells within the naive and memory B cell subsets from at least 5 healthy donors analyzed in duplicates - quadruplicates. ****p<0.0001; ns, not significant (2-way Anova with Tukey multiple comparisons test).

D. BAFF induces phosphorylation of the translational repressor 4E-BP1 in naive but not in memory B cells.

Naive and memory B cells were treated with

BAFF or CD40L overnight. Whole cell extracts were immunoblotted with antibodies against total and phosphorylated 4E-BP1 (S65). Data are representative of one out of two independent experiments. N-fold changes in p4E-BP1 and 4E-BP1 levels were calculated as signals normalized to actin and further normalized to the untreated sample from day 0 for each B cell subset.

E. *TCL1A* inactivation in DG-75 cells. DG-75 cells were electroporated with a gRNA-Cas9 RNP complex targeting the exon 1 of the *TCL1A* locus. Total *TCL1A* protein expression in the parental DG-75 cells and *TCL1A* KO cells was assessed by western blotting. The position of *TCL1A* in the western blot is marked by the arrow.

F. *TCL1A* inactivation impairs BAFF-induced upregulation of CD69. *TCL1A* was inactivated in primary B cells as in DG-75 (shown in E). Two days after the electroporation, cells were incubated with BAFF (20 ng/mL) or without for one day and analyzed for the expression of CD69 by IgD⁺ CD27⁻ naive B cells. The histogram plots show the percentage of *TCL1A*-negative cells, which increased from 21% in mock electroporated cells to 47% in B cells electroporated with *TCL1A* gRNA/Cas9 RNPs. The graph shows the n-fold changes in the percentages of CD69⁺ cells in response to BAFF treatment of *TCL1A*-negative and *TCL1A*-positive, mock-electroporated or *TCL1A*-inactivated cells after one day of cultivation ± BAFF. BAFF did not induce CD69 expression in *TCL1A*⁻ naive B cells. The experiment shows 2 - 4 independent replicates of two different donors. Significant differences were calculated by two-tailed Brown-Forsythe and Welch ANOVA for multiple comparisons assuming unequal SDs (ns = not significant. * p<0.0332; ** p<0.0002; ns, not significant).

G. Inhibition of PI3K reduces upregulation of CD69. IgD⁺ CD27⁻ naive B cells were cultivated overnight without or with BAFF in the presence of the PI3K inhibitor nemiralisib (iPI3K, 1 μ M) or DMSO and analyzed for the surface expression of CD69 by flow cytometry. The plot shows the mean \pm SD of the percentage of CD69⁺ cells within the naive subset. * p <0.05; ns: not significant (2-way ANOVA with Sidak's multiple comparisons test).

H. *TCL1A* inactivation does not change BAFF-induced survival. *TCL1A* was inactivated in B cells as described in the legend of panel E. Two days post electroporation, cells were cultivated without or with BAFF (20 ng/ml) for 3 additional days. Survival of total and *TCL1A*⁻ IgD⁺ CD27⁻ naive cells was analyzed by flow cytometry and timed acquisition. The experiment was performed in 5 - 9 technical replicates. **** p <0.0001; ** p <0.01; ns, not significant (2-way ANOVA with Tukey multiple comparisons test).

I. *BCL-2*, *BCL-XL* and *MCL-1* mRNA levels in naive and memory B cells. B cell subsets were cultivated for 6 h with BAFF (20 ng/mL) or left untreated; transcript levels were analyzed by RNA-Seq as described in Figure 2. The box plots represent the normalized gene expression values showing the spread as boxes, means as lines, and the individual values as dots. The numerical values correspond to the means.

K. Inhibition of PI3K and NIK prevents BAFF-induced *BCL-2* expression in naive B cells. B cells were cultivated for 2 days with BAFF (20 ng/mL) in the presence of inhibitors against PI3K δ (nemiralisib, 0.625 μ M), NIK (SMI1, 10 μ M) or DMSO (control) and analyzed for *BCL-2* expression by intracellular flow cytometry. The plot shows the mean and SEM of *BCL-2* MFI in naive and MBCs from two independent experiments with two different HD and technical duplicates.

**** $p < 0.0001$; ** $p < 0.01$; ns, not significant (2-way ANOVA with Tukey multiple comparisons test).

L. PI3K inhibition interferes with BAFF-induced expression of anti-apoptotic proteins MCL-1 and BCL-XL in naive B cells. Western blot analysis of MCL-1 and BCL-XL in naive and memory B cells after an overnight stimulation with BAFF or CD40L in the presence of inhibitors against PI3K δ , NIK or DMSO (control). The immunoblot shows the representative data from one out of two independent experiments. N-fold change of MCL-1 and BCL-XL expression was calculated as signals normalized to actin and further normalized to the untreated sample for each B cell subset.

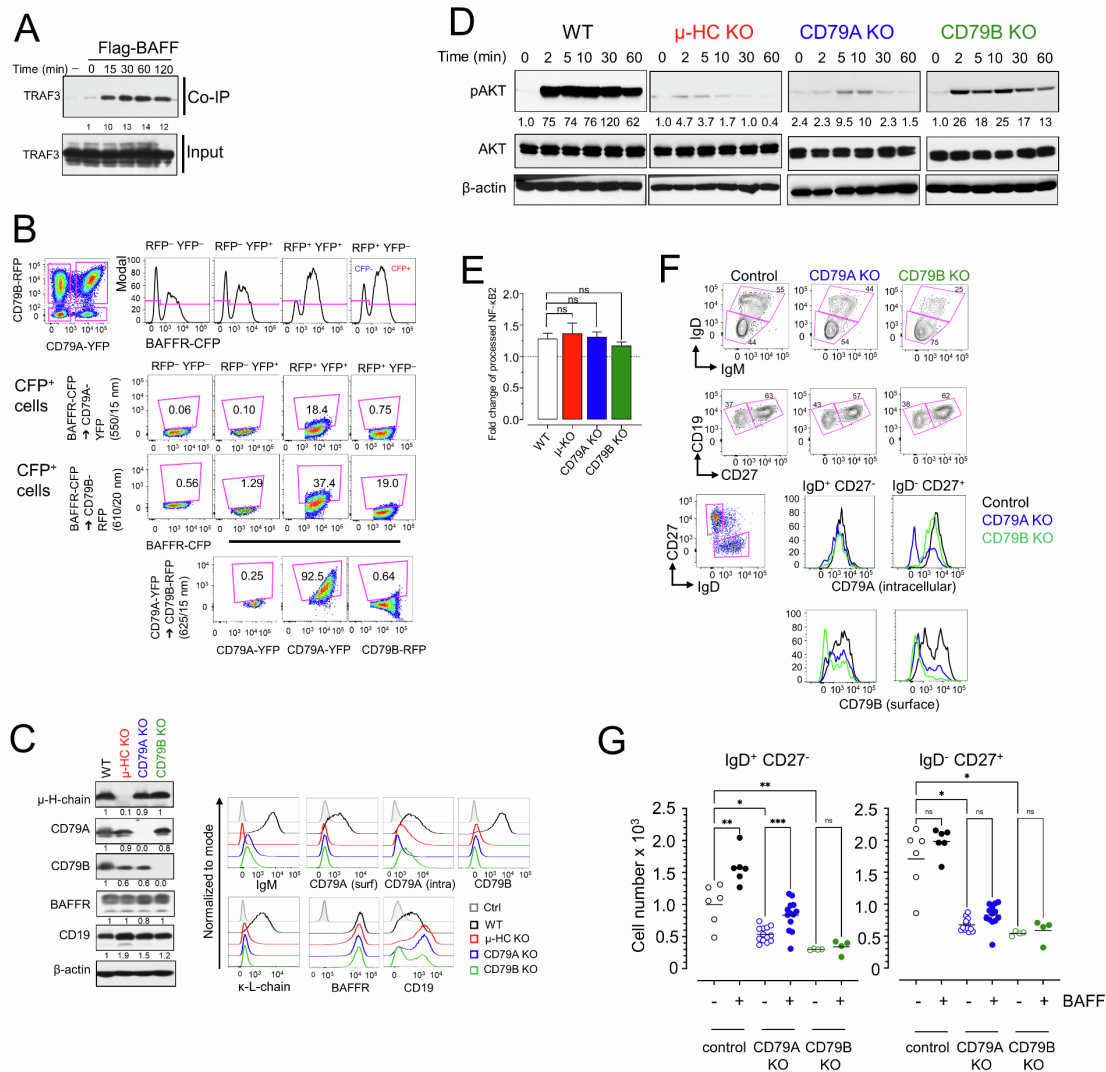


Figure S4 (related to Figure 5). Interactions with BCR components regulate BAFFR signaling.

A. FLAG-BAFF co-immunoprecipitates TRAF3. DG-75 cells were incubated with FLAG-tagged BAFF for 15 - 120 min at 37°C or at 0°C for 5 min ($t = 0$). Cells were lysed and immunocomplexes were precipitated with anti-FLAG M2-coupled agarose beads followed by western blot analysis of TRAF3. Lysates of untreated cells were used as control (-) to determine non-specific binding of proteins to the beads. N-fold change in TRAF3 recruitment was calculated as signals normalized to TRAF3 in input samples and further normalized to $t = 0$.

B. Gating strategy to detect FRET⁺ cells. BAFFR-KO DG-75 Burkitt's lymphoma cells were transduced with lentiviral vectors encoding BAFFR-CFP, CD79A-YFP and CD79B-RFP fusion proteins. The transduction resulted in 4 populations according to YFP/RFP expression: RFP⁺ cells, YFP⁺ cells, YFP⁺ RFP⁺ cells and YFP⁻ RFP⁻ cells. Based on the expression of BAFFR-CFP, each subset was divided into CFP⁺ and CFP⁻ cells (histogram plots of upper row, RFP⁺ YFP⁻, RFP⁺ YFP⁺, RFP⁻ YFP⁺ and RFP⁻ YFP⁻ cells showing expression of BAFFR-CFP). FRET from CFP to YFP or from CFP to RFP was detected in the CFP⁺ subsets, whereas FRET from YFP to RFP was only detected in the YFP⁺ RFP⁺ population. Excitation of CFP with the 405 nm laser induced fluorescence resonance energy transfer from CFP to YFP which was detected using a 550/15 nm bandpass filter (BAFFR-CFP → CD79A-YFP 550/15 nm). Energy transfer from CFP excited by the 405 nm laser to RFP was detected by signals passing a 610/20 nm bandpass filter (BAFFR-CFP → CD79B-RFP 610/20 nm). Energy transfer from YFP excited by 488 nm laser to RFP was detected using an 625/15 nm band pass filter (bottom row). Cell populations which did not express the respective FRET partner protein (YFP⁻ RFP⁻ cells, YFP⁺ RFP⁻ cells and RFP⁺ YFP⁻ cells) were used to set the gates for FRET⁺ cells. In particular, to detect FRET from CFP to YFP or RFP, CFP⁺ YFP⁻ RFP⁻ cells were used to set the gates for signals passing the 550/15 nm and the 610/20 nm filters, while the CFP⁻ YFP⁺ RFP⁻ cells were used to set the gate for signals passing the 625/15 nm filter.

C. CD79A-, CD79B- and μ -H chain KO DG-75 cells. Western blot analysis of whole cell lysates from wild-type (WT), μ -H-chain (μ -HC), CD79A and CD79B KO cells showing total expression of μ -H-chain, CD79A, CD79B, BAFFR and CD19; β -actin was used as a loading control; n-fold differences in protein expression

were calculated as signals normalized to actin and further normalized to the WT DG-75 cells (left panels). Flow cytometric analysis of surface expression of IgM, CD79A, CD79B, kappa light chain, BAFFR, CD19 and intracellular expression of CD79A in the WT, μ -H-chain, CD79A and CD79B KO DG-75; control = unstained cells (right panels).

D. Time course of AKT phosphorylation (S473) in response to anti-IgM treatment in WT, μ -H-chain, CD79A and CD79B KO DG-75 cells. Cells were treated with F(ab')₂ anti-IgM (2 μ g/mL) for 2 - 60 min. Whole cell extracts were analyzed by western blot using antibodies against pAKT (S473), total AKT and β -actin (loading control), showing that loss of CD79A, CD79B or μ -H chain prevents AKT phosphorylation. Data are representative of 1 out of at least 5 independent experiments. N-fold changes were calculated relative to the t=0 sample of WT DG-75 cells.

E. NF- κ B2 activation in CD79A, CD79B and μ -H-chain KO DG-75 cells. DG-75 (WT), CD79A, CD79B and μ -H-chain KO cells were pre-treated overnight with an inhibitor against NIK (10 μ M) to reduce the basal NF- κ B2 processing. Then, the inhibitor was washed out and the cells were stimulated with BAFF (100 ng/mL) overnight in inhibitor-free medium. The next day, whole cell lysates were prepared to detect NF- κ B2 processing by western blot. The percentage of processed NF- κ B2 was calculated as $[(\text{signal of p52})/(\text{signal of p52} + \text{signal of p100})] \times 100$. The plot depicts the mean and SEM of n-fold changes in processed NF- κ B2 after the addition of BAFF in the different cell lines from at least 3 independent experiments with 2 technical replicates. ns, not significant (Kruskal-Wallis test with Dunn's correction).

F. Gene inactivation of *CD79A* and *CD79B* in primary human B cells. *CD79A* and *CD79B* were inactivated by Cas9-directed mutagenesis in purified B cells with *CD79A* and *CD79B* gRNA-Cas9 RNPs. Equal numbers of cells were distributed into technical replicates, cultivated for 5 days and analyzed by flow cytometry and timed acquisition. Analysis of CD19⁺ cells for IgM, IgD, and CD27 expression revealed a decrease in IgM and IgD surface levels after inactivation of *CD79A* and *CD79B* (contour plots). The inactivation of *CD79A* also reduced the surface expression of *CD79B* in both IgD⁺ CD27⁻ and IgD⁻ CD27⁺ cells. The pseudocolor plot shows the gating and the histogram overlays of *CD79A* and *CD79B* expression in mock electroporated controls (black), in *CD79A* KO (blue) and *CD79B* KO B cells (green).

G. BAFF does not rescue B cells after inactivation of *CD79B*. B cells were electroporated with gRNA/Cas9 RNPs targeting *CD79A* (blue symbols) or *CD79B* (green symbols), or without RNP complex (control, black symbols). Two days post electroporation, cells were cultivated ±BAFF (20 ng/ml) and analyzed by flow cytometry and timed acquisition after 3 additional days. The plots show the cell numbers of IgD⁺ CD27⁻ and IgD⁻ CD27⁺ cells from 2 HD (≥4 independent replicates). Because the inactivation of *CD79A* is less efficient than the inactivation of *CD79B*, some of the naive B cells in the *CD79A* KO samples are rescued by BAFF. The number of mock-electroporated or of *CD79A* or *CD79B* KO IgD⁻ CD27⁺ MBCs did not change in response to BAFF. ***p<0.0002; **p<0.0021; *p<0.0332; ns, not significant (Brown-Forsythe and Welch's ANOVA test for multiple comparisons).

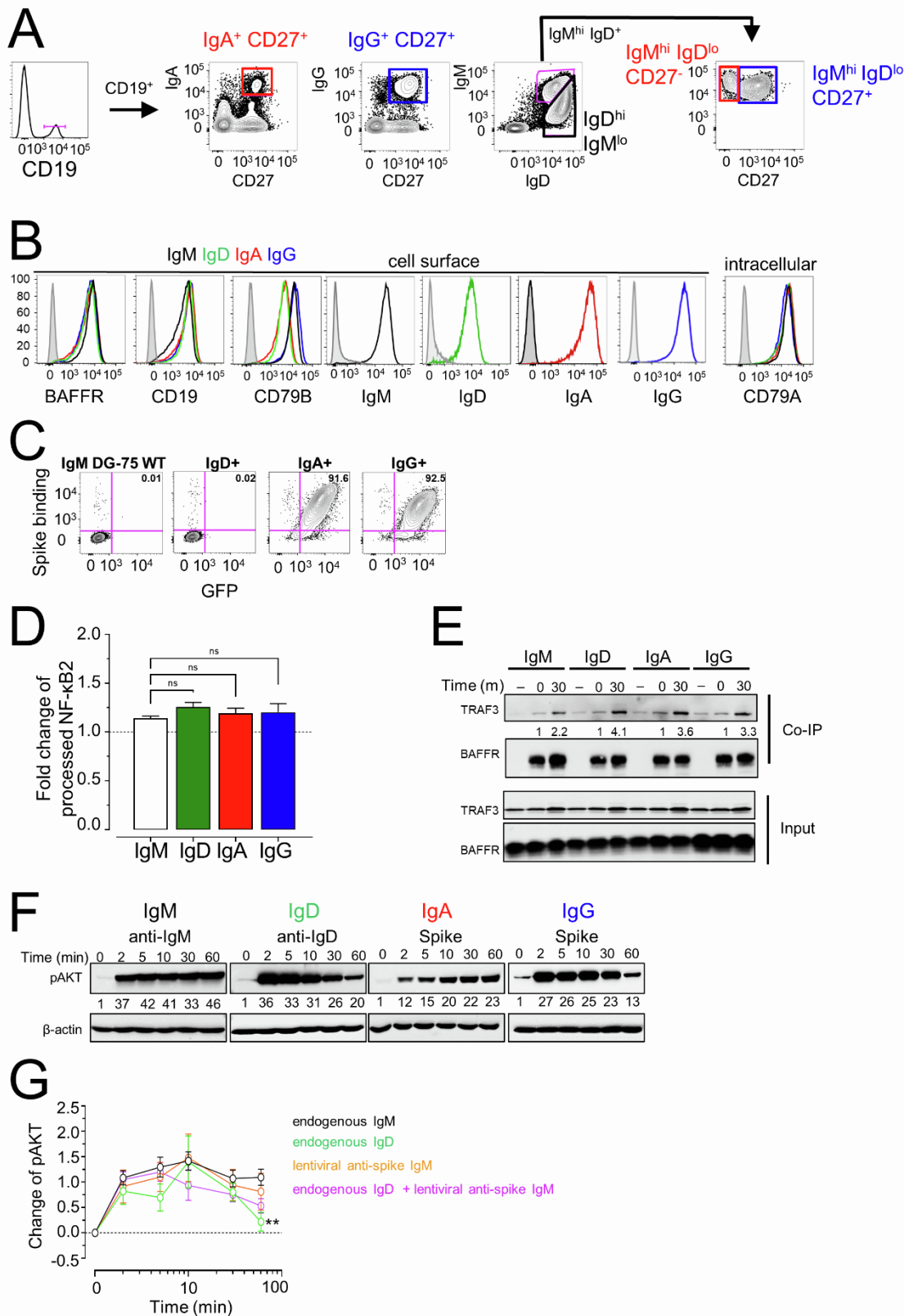


Figure S5 (related to Figure 6). The BCR isotype restricts BAFF-induced PI3K activation in naive B cells.

A. Flow cytometric analysis of B cell subsets expressing different immunoglobulin isotypes. CD19⁺ cells were gated according to the expression of IgM, IgD, IgG, IgA and CD27 into IgD^{hi} IgM^{low} CD27⁻, IgD^{low} IgM^{hi} CD27⁻, IgD^{low} IgM^{hi} CD27⁺, IgA⁺ CD27⁺, and IgG⁺ CD27⁺ subsets and analyzed by flow cytometry for the surface expression of Ig-kappa and Ig-lambda light chains shown in Figure 6.

B. Surface expression of BAFFR, CD19, CD79B, IgM, IgD, IgA, IgG and intracellular expression of CD79A in DG-75 cell lines with different BCR isotypes. Grey histogram = unstained cells.

C. Binding of SARS-CoV-2 spike antigen to DG-75 cell lines expressing anti-spike IgA or IgG. DG-75 WT (IgM⁺), IgD⁺, anti-spike IgA1⁺ and IgG1⁺ DG-75 cell lines (GFP⁺) were incubated with His-tagged-SARS-CoV-2 spike protein (1 µg/mL) for 30 min on ice. Cells were washed and further incubated with an anti-His tag Alexa Fluor 647-conjugated antibody for 30 min on ice. Cells were washed and analyzed by flow cytometry.

D. NF-κB2 activation in DG-75 cells expressing different BCR isotypes. Cells were treated overnight with an inhibitor against NIK (10 µM) to reduce the basal NF-κB2 processing. The day after, the inhibitor was washed out and the cells were treated with BAFF (100 ng/mL) overnight in inhibitor-free medium. The next day, whole cell lysates were prepared and NF-κB2 processing was analyzed by western blot. Signal intensities were determined by densitometry and the processing of NF-κB2 p100 into p52 was determined as [(signal of p52)/(signal of p100+ signal of p52)] x 100. The plot depicts the mean and SEM of fold change in p52 levels after the addition of BAFF. Data are pooled from 3 independent

experiments (2 technical replicates/experiment). ns, not significant (Kruskal-Wallis test with Dunn's correction).

E. Similar TRAF3 recruitment to BAFFR in B cell lines expressing different isotypes. DG-75 cells expressing IgM, IgD, IgA1, or IgG1 isotypes were incubated for 0 - 30 min with FLAG-tagged BAFF followed by co-immunoprecipitation with anti-FLAG M2 mAb-coupled agarose beads and western blot analysis for TRAF3 and BAFFR. Immunoprecipitates of untreated cells (-) were used as control for unspecific binding. N-fold changes of TRAF3 were calculated as signals normalized to BAFFR and further normalized to the sample treated with BAFF for 5 min on ice (t=0) per each cell line.

F. Kinetics of AKT phosphorylation (S473) in B cell lines expressing different isotypes in response to BCR activation. Cells were incubated with F(ab')₂ anti-IgM (2 µg/mL), F(ab')₂ anti-IgD (2 µg/mL), or recombinant SARS-CoV-2 spike protein (1µg/mL) for 2 - 60 min and analyzed by western blot for pAKT (S473); β-actin was used as a loading control. The western blots are representative of ≥2 independent experiments. N-fold changes were calculated relative to the t=0 sample of each cell line.

G. Similar kinetics of AKT phosphorylation (S473) in B cell lines expressing anti-spike IgM and native IgM and IgD BCRs. DG-75 cells expressing native IgM or IgD, anti-spike IgM or dual positive cells (native IgD/anti-spike IgM) were treated with BAFF (100 ng/mL) for 2 - 60 min and analyzed by western blot for pAKT (S473). After densitometric analysis of signal intensities, the changes in pAKT signals were calculated as [(signal t_x-signal t₀)/signal t₀]. Plot shows the mean and SEM of ≥5 independent experiments. **p<0.01 (Mann-Whitney test)

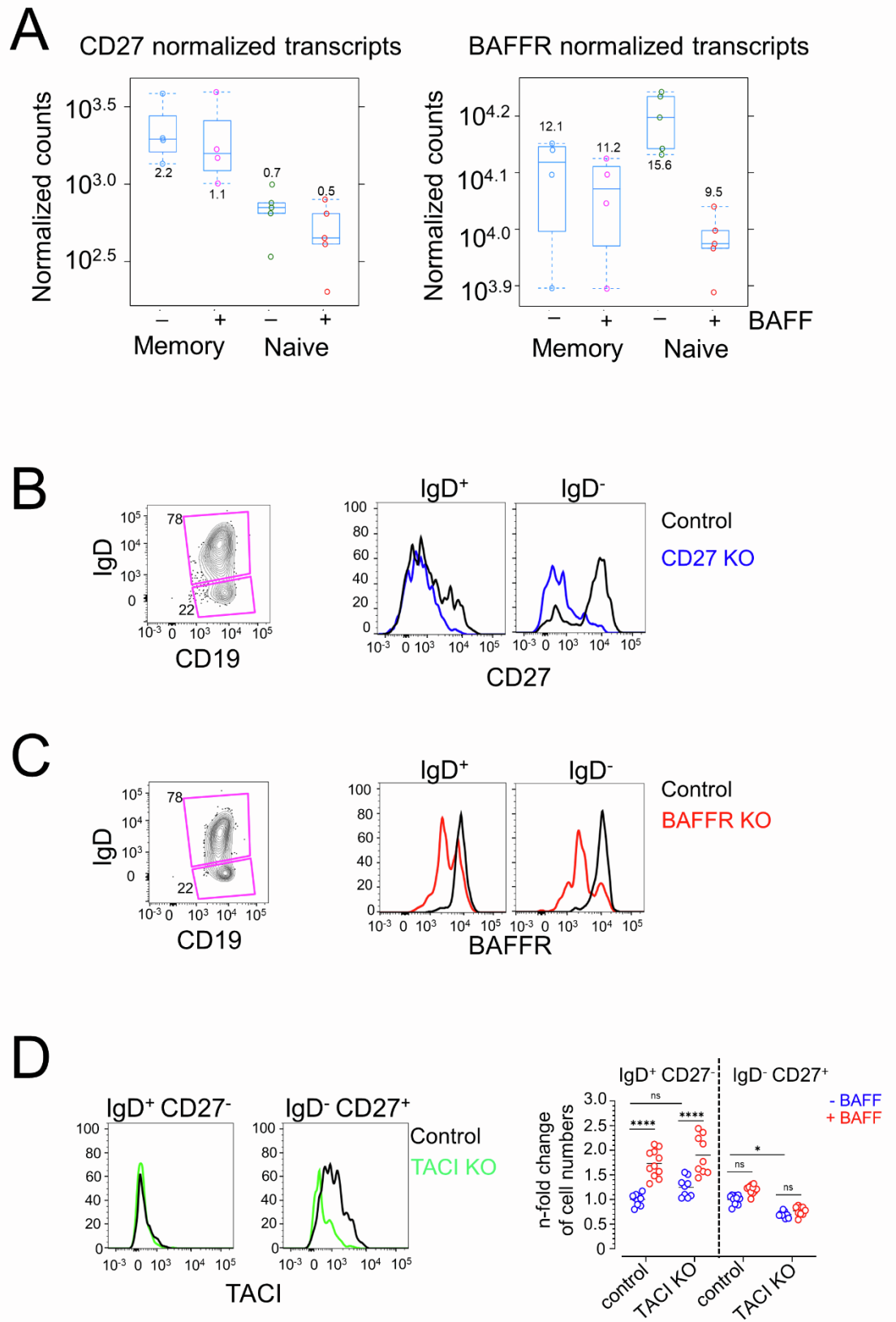


Figure S6 (related to Figure 7). Inactivation of *CD27* and *BAFFR* in primary B cells.

A. Levels of *CD27* and *BAFFR* transcripts expressed by naive and switched memory B cells. Naive and memory B cells were cultivated with BAFF (20 ng/mL) or left untreated for 6 h as described in Figure 2. The box plots represent the normalized gene expression showing the spread as boxes, means (numerical values) as lines, the individual values as dots. RNA-Seq was performed as described in Figure 2.

B. Inactivation of *CD27* by CRISPR-Cas9. B cells were electroporated with a *CD27*-gRNA/Cas9 RNP complex or without an RNP complex (control). Cells were cultivated for 5 days and analyzed by flow cytometry for the expression of *CD27*. *CD19*⁺ B cells were gated according to the expression of *IgD* into *IgD*⁺ (naive and MZ) and *IgD*⁻ memory B cells.

C. Inactivation of *TNFRSF13C* in human B cells. Cells were electroporated with a gRNA-Cas9 RNP complex targeting the exon 2 of the *TNFRSF13C* gene. Cells electroporated under the same conditions without a gRNA-Cas9 RNP complex served as controls. Electroporation of B cells with the *BAFFR*-gRNA/Cas9 RNP complex resulted in > 50% reduction of *BAFFR* expression in naive and MZ (*IgD*⁺) B cells and in >70% in memory (*IgD*⁻) B cells after 5 days of cultivation.

D. Loss of *TACI* does not restore responsiveness of memory B cells to *BAFF*. B cells were electroporated with a *TACI*-gRNA/Cas9 RNP complex or without an RNP complex (control) and analyzed by flow cytometry and timed acquisition. (left) Histogram overlays show *TACI* expression in *IgD*⁺ *CD27*⁻ (naive) and *IgD*⁻ *CD27*⁺ (memory) B cells at day 5. (right) Loss of *TACI* does not affect *BAFF*-induced survival of B cell subsets. At day 2 after electroporation, cells were treated with *BAFF* (20 ng/ml) or left untreated for additional 3 days. Cell numbers

were evaluated by flow cytometry and timed acquisition. N-fold change in cell numbers was calculated as [cell numbers \pm gTACI-RNP \pm BAFF/cell numbers wo RNP wo BAFF] per each subset. Plot shows the mean of two independent experiments with two healthy donors (≥ 4 replicates per condition). **** $p < 0.0001$; * $p < 0.05$; ns, not significant (2-way ANOVA with Tukey multiple comparisons test).